blood®
Regular Article

Check for updates

LYMPHOID NEOPLASIA

Genetic drivers of oncogenic pathways in molecular subgroups of peripheral T-cell lymphoma

Tayla B. Heavican,[1,*] Alyssa Bouska,[1,*] Jiayu Yu,[1] Waseem Lone,[1] Catalina Amador,[1] Qiang Gong,[2] Weiwei Zhang,[1] Yuping Li,[2] Bhavana J. Dave,[1,3] Maarja-Liisa Nairismägi,[4] Timothy C. Greiner,[1] Julie Vose,[5] Dennis D. Weisenburger,[2] Cynthia Lachel,[5] Chao Wang,[1,2] Kai Fu,[1] Jadd M. Stevens,[3] Soon Thye Lim,[4] Choon Kiat Ong,[4] Randy D. Gascoyne,[6] Edoardo Missiaglia,[7] Francois Lemonnier,[8] Corinne Haioun,[8] Sylvia Hartmann,[9] Martin Bjerregård Pedersen,[10] Maria Antonella Laginestra,[11] Ryan A. Wilcox,[12] Bin Tean Teh,[4] Noriaki Yoshida,[13] Koichi Ohshima,[13] Masao Seto,[13] Andreas Rosenwald,[14] German Ott,[15] Elias Campo,[16] Lisa M. Rimsza,[17] Elaine S. Jaffe,[18] Rita M. Braziel,[19] Francesco d'Amore,[10] Giorgio Inghirami,[20] Francesco Bertoni,[21] Laurence de Leval,[7] Philippe Gaulard,[8] Louis M. Staudt,[22] Timothy W. McKeithan,[2] Stefano Pileri,[11] Wing C. Chan,[2] and Javeed Iqbal[1]

[1]Pathology and Microbiology, University of Nebraska Medical Center, Omaha, NE; [2]Department of Pathology, City of Hope National Medical Center, Duarte, CA; [3]Human Genetics Laboratory, University of Nebraska Medical Center, Omaha, NE; [4]Division of Medical Oncology, National Cancer Centre Singapore, Singapore; [5]Division of Hematology and Oncology, University of Nebraska Medical Center, Omaha, NE; [6]Center for Lymphoid Cancer, British Columbia Cancer Agency, Vancouver, BC, Canada; [7]Institute of Pathology, Lausanne University Hospital, Lausanne, Switzerland; [8]Département de Pathologie, Université Paris-Est, Hôpital Henri-Mondor, INSERM U955, Créteil, France; [9]Senckenberg Institute of Pathology, Goethe University, Frankfurt am Main, Germany; [10]Department of Hematology, Aarhus University Hospital, Aarhus, Denmark; [11]European Institute of Oncology, Milan/Bologna University School of Medicine, Bologna, Italy; [12]Department of Internal Medicine, University of Michigan Rogel Cancer Center, Ann Arbor, MI; [13]Department of Pathology, Kurume University School of Medicine, Fukuoka, Japan; [14]Institute of Pathology, University of Wuerzburg and Comprehensive Cancer Center Mainfranken, Wuerzburg, Germany; [15]Department of Clinical Pathology, Robert-Bosch-Krankenhaus and Dr. Margarete Fischer-Bosch Institute of Clinical Pharmacology, Stuttgart, Germany; [16]Hematopathology Unit, Hospital Clinic, Barcelona, Spain; [17]Department of Pathology, University of Arizona, Tucson, AZ; [18]Laboratory of Pathology, Center for Cancer Research, National Cancer Institute, National Institutes of Health, Bethesda, MD; [19]Oregon Health Sciences Center, Portland, OR; [20]Department of Pathology and NYU Cancer Center, New York University School of Medicine, New York, NY; [21]Università della Svizzera Italiana, Istituto Oncologico di Ricerca, Bellinzona, Switzerland; and [22]Metabolism Branch, Center for Cancer Research, National Cancer Institute, National Institutes of Health, Bethesda, MD

KEY POINTS

- **Chr5 and chr21 gains co-occurred with *IDH2*^{R172} mutation in AITL, whereas *IDH2* wild-type cases had deletions targeting PI3K–AKT–mTOR.**
- **PTCL-NOS molecular subgroups (PTCL-GATA3 and PTCL-TBX21) had distinct genetic aberrations, and *CDKN2A* loss showed prognostic significance.**

Peripheral T-cell lymphoma (PTCL) is a group of complex clinicopathological entities, often associated with an aggressive clinical course. Angioimmunoblastic T-cell lymphoma (AITL) and PTCL-not otherwise specified (PTCL-NOS) are the 2 most frequent categories, accounting for >50% of PTCLs. Gene expression profiling (GEP) defined molecular signatures for AITL and delineated biological and prognostic subgroups within PTCL-NOS (PTCL-GATA3 and PTCL-TBX21). Genomic copy number (CN) analysis and targeted sequencing of these molecular subgroups revealed unique CN abnormalities (CNAs) and oncogenic pathways, indicating distinct oncogenic evolution. PTCL-GATA3 exhibited greater genomic complexity that was characterized by frequent loss or mutation of tumor suppressor genes targeting the *CDKN2A/B-TP53* axis and *PTEN*-PI3K pathways. Co-occurring gains/amplifications of *STAT3* and *MYC* occurred in PTCL-GATA3. Several CNAs, in particular loss of *CDKN2A*, exhibited prognostic significance in PTCL-NOS as a single entity and in the PTCL-GATA3 subgroup. The PTCL-TBX21 subgroup had fewer CNAs, primarily targeting cytotoxic effector genes, and was enriched in mutations of genes regulating DNA methylation. CNAs affecting metabolic processes regulating RNA/protein degradation and T-cell receptor signaling were common in both subgroups. AITL showed lower genomic complexity compared with other PTCL entities, with frequent co-occurring gains of chromosome 5 (chr5) and chr21 that were significantly associated with *IDH2*^{R172} mutation. CN losses were enriched in genes regulating PI3K–AKT–mTOR signaling in cases without *IDH2* mutation. Overall, we demonstrated that novel GEP-defined PTCL subgroups likely evolve by distinct genetic pathways and provided biological rationale for therapies that may be investigated in future clinical trials. (*Blood*. 2019;133(15):1664-1676)

Introduction

Peripheral T-cell lymphoma (PTCL) accounts for 10% to 15% of non-Hodgkin lymphomas (NHLs) in the western world and ~20% of NHLs in Asia or Central and South America.[1] The current World Health Organization (WHO) classification recognizes ~30 distinct PTCL entities, including angioimmunoblastic T-cell lymphoma (AITL), anaplastic large cell lymphoma (ALCL), adult T-cell leukemia/lymphoma (ATLL) and extranodal NK/T-cell lymphoma

Downloaded from http://ashpublications.org/blood/article-pdf/133/15/1664/1553089/blood872549.pdf by guest on 29 April 2025

of nasal type with distinct clinicopathological characteristics.[1] PTCL patients exhibit poor response to standard chemotherapy,[2] with the exception of ALK- and *DUSP22*-translocated ALCL cases.[3] AITL is the most common PTCL entity, with distinct clinicopathological features,[4,5] including a dysregulated immune system evidenced by polyclonal hypergammaglobulinemia and autoimmune manifestations, while also displaying strong immunosuppression in the tumor with the frequent presence of Epstein-Barr virus–infected B cells.[4] We and other investigators have demonstrated T follicular helper (T_{FH}) cells as the cell of origin and characteristic activation of the NF-κB pathway.[6-8] AITL has frequent mutations of genes regulating the epigenome (*TET2*, *IDH2*^{R172}, and *DNMT3A*) and proximal T-cell receptor (TCR) and costimulatory signaling pathways.[9-13] However, the complex underlying pathobiology of AITL remains poorly defined.

Approximately 30% to 50% of PTCL cases cannot be further classified and are designated PTCL-not otherwise specified (PTCL-NOS).[1,2] Thus, PTCL-NOS includes a heterogeneous group of cases that is difficult to diagnose and treat.[2] Using gene expression profiling (GEP), we identified diagnostic and prognostic molecular signatures for major PTCL entities and identified 2 novel molecular subgroups within PTCL-NOS.[7,8,14] These subgroups were characterized by differential expression of master T helper 1 (T_H1) or T_H2 cell-differentiation regulators (*TBX21* or *GATA3*, respectively) with corresponding target genes[8,15] and significant differences in oncogenic transcriptional signatures and clinical outcome.[8] Although these subgroups have been alluded to in the 2017 WHO classification scheme,[1] the genetic basis of this distinction is unknown. We investigated the genetic etiology of the subgroups using extensive GEP, genomic copy number (CN) analysis, and mutation analysis of candidate driver genes within abnormal loci. Furthermore, we evaluated potential therapeutic targets affecting oncogenic pathways in these molecular subgroups.

Materials and methods

Detailed materials and methods can be found in supplemental Materials and methods (available on the *Blood* Web site).

Patient material and cell lines

Data for AITL (n = 35) and PTCL-NOS (n = 69) are shown in supplemental Table 1. We removed PTCL-T_{FH} cases[16] (n = 15) from PTCL-NOS using messenger RNA (mRNA) or protein (immunohistochemistry [IHC]) markers of T_{FH} cells (Figure 1A-B; supplemental Table 1). A total of 114 (of 119) PTCL cases were reviewed by ≥2 hematopathologists for consensus diagnosis. All but 14 cases have been characterized previously.[7,8,17,18] Genomic data from ATLL,[19] ALCL,[20] cutaneous T-cell lymphoma (CTCL),[21] and PTCL-NOS[17,22,23] were evaluated for identification of subtype-specific CN abnormalities (CNAs). Characteristics of the T-cell lines are shown in supplemental Table 2.

Genomic CN analysis

Affymetrix SNP-250K (n = 12), SNP 6.0 (n = 8), OncoScan (n = 71), and Agilent SurePrint[17] (n = 25) arrays were used (supplemental Table 1). CNAs were analyzed with Nexus Copy Number (BioDiscovery). To ensure appropriate platform integration, 6 cases were profiled on both the SNP-250K and OncoScan platforms, and highly concordant CN profiles were observed. Tumor content was assessed by the ABSOLUTE algorithm[24] based on single nucleotide polymorphism hybridization and by morphologic review of the percentage of pleomorphic neoplastic T cells in cases with material available for review. We did not detect significant correlation between high or low aberrant genomes and tumor content, suggesting that detection of fewer CNAs cannot be explained simply by low tumor content (supplemental Table 1).

CN profiles from European (Affymetrix SNP-250K, n = 47)[22] and Asian (bacterial artificial chromosome array, n = 51)[23] PTCL-NOS cohorts were reevaluated for meta-analysis. These cohorts showed genomic profiles similar to the current datasets (supplemental Figure 1A-D).

Molecular classification of cases with RNA-seq and FFPE-derived GEP data

A predefined GEP signature for AITL[8] was used to evaluate pathological AITL cases with RNA sequencing (RNA-seq) data. Eight cases with RNA-seq data were molecularly classified as AITL with >80% probability using a Bayesian algorithm (supplemental Figure 2A). A similar analysis was performed for PTCL-GATA3 and PTCL-TBX21 subtyping for formalin-fixed paraffin-embedded (FFPE) samples[7,8] (supplemental Figure 2B).

Integrative analysis of CNAs and GEP

mRNA expression and CN status were compared using a 1-sided Student *t* test. Ingenuity pathway analysis and DAVID were used for integrated pathway analysis of the genes within aberrant loci.

Unsupervised hierarchical clustering

Unsupervised hierarchical clustering (HC) of PTCL-NOS cases by the CN status of recurrent abnormalities (≥10% frequency in PTCL-GATA3 or PTCL-TBX21) was performed with Cluster 3.0.

Target gene sequencing and analysis

A SureSelect panel (Agilent) targeting 334 genes mutated in NHLs and encompassing aberrant loci was used for mutational analysis. Libraries were sequenced using an Illumina system. Data analysis was described previously.[25]

Results

Clinical characteristics and molecular classification of PTCL

PTCL cases were classified using our predefined GEP signatures.[7,8] These included fresh-frozen (FF) tissues (n = 94) profiled by HG-U133 Plus2,[7,8,17] FFPE tissues (n = 17) profiled using DASL (Illumina),[18] and 8 AITL cases with RNA-seq data (supplemental Figure 2). PTCL-T_{FH} cases (n = 15), a provisional entity according to the 2017 WHO classification,[1] were identified primarily by morphological assessment and the expression of the WHO-defined IHC markers.[1] However, 6 cases lacking tissue for IHC were identified based on a recently described PTCL-T_{FH} GEP signature,[17] which showed mRNA expression similar to known PTCL-T_{FH} samples (Figure 1A-B). When we examined the T_{FH} signature[17] in the entire set, it was found to be enriched in only AITL or PTCL-T_{FH} (Figure 1B). After excluding PTCL-T_{FH} cases, PTCL-NOS cases were subclassified into PTCL-GATA3 (n = 31) and PTCL-TBX21 (n = 30) subgroups using GEP, and 5 cases remained unclassifiable.[7,8] PTCL-T_{FH} cases were used only for comparative analysis (supplemental Figure 1E). There was no significant difference in age between cohorts (supplemental

Downloaded from http://ashpublications.org/blood/article-pdf/133/15/1664/1553089/blood872549.pdf by guest on 29 April 2025

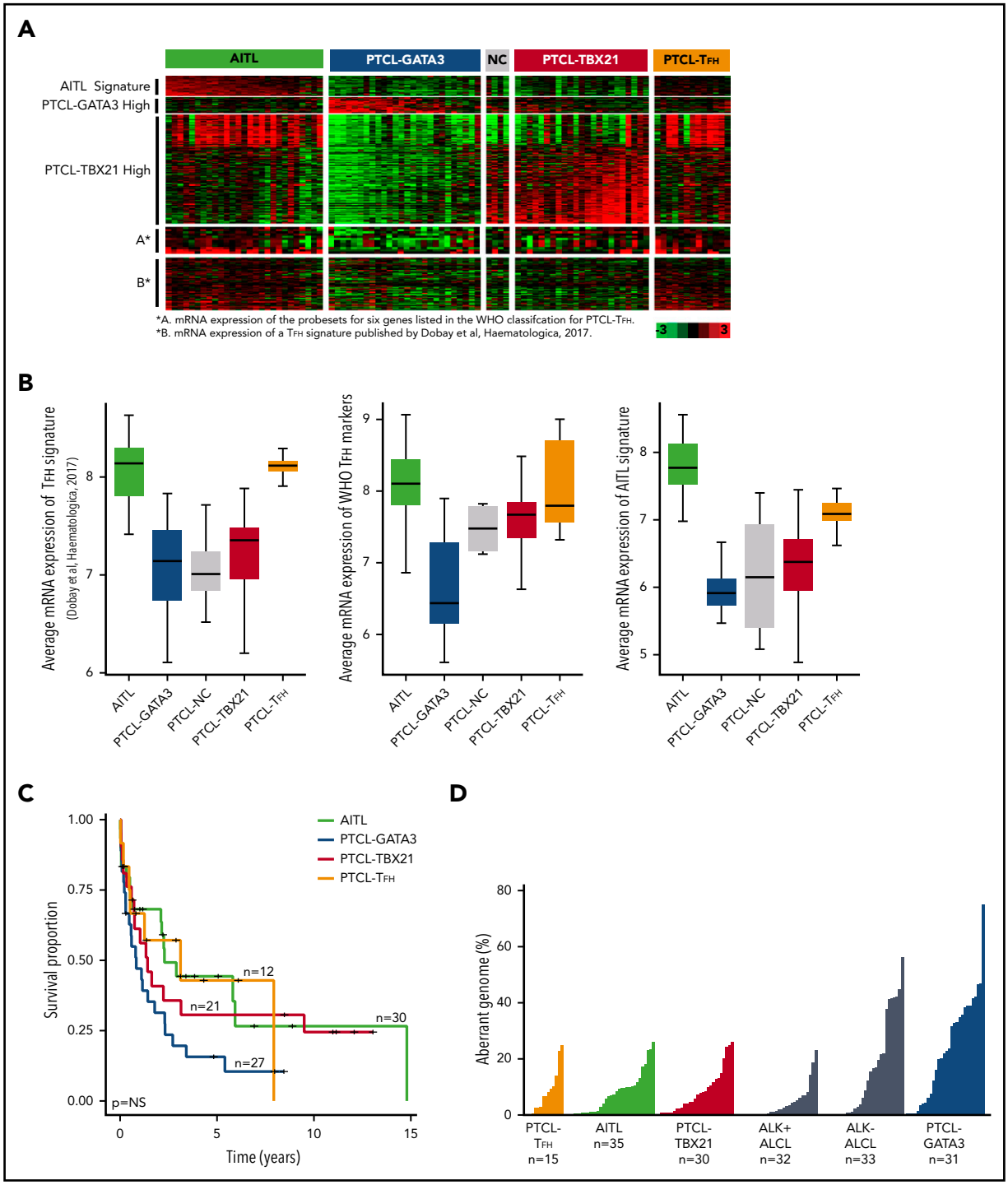

Figure 1. Characteristics of PTCL entities and subgroups. (A) Gene expression data of predefined gene signatures for AITL, the PTCL-GATA3 and PTCL-TBX21[8] subgroups, and PTCL-T_{FH}[17] using fresh-frozen RNA on the HG-U133 Plus2 platform (Affymetrix). (B) Average expression of the PTCL-T_{FH} signature[17] in PTCL subgroups (left panel), the probe sets for 6 genes listed by the WHO to classify PTCL-T_{FH} (middle panel), and the AITL molecular signature[8] (right panel). (C) Kaplan-Meier curves comparing OS between the PTCL subgroups with available data. (D) Comparison of percent aberrant genome in PTCL subgroups (PTCL-T_{FH}, AITL, PTCL-TBX21, ALK^+ ALCL,[20] ALK^- ALCL,[20] and PTCL-GATA3).

Table 3). PTCL-GATA3 showed inferior overall survival (OS) compared with other groups (Figure 1C), as previously demonstrated.[8,15]

Integrated genomic analysis of molecularly defined AITL

AITL had the least abnormal genome (mean = 7%), with CN gains more frequent than CN losses and with a percent aberrant genome comparable to PTCL-T_{FH} and PTCL-TBX21 (Figure 1D). Cases with low aberrant genomes showed no significant difference in tumor content compared with highly aberrant cases, as estimated by the ABSOLUTE algorithm based on single nucleotide polymorphism hybridization,[24] as well as by morphologic review of the percentage of neoplastic T cells. This suggests that detection of fewer CNAs was not due to low tumor content (supplemental Table 1).

Downloaded from http://ashpublications.org/blood/article-pdf/133/15/1664/1553089/blood872549.pdf by guest on 29 April 2025

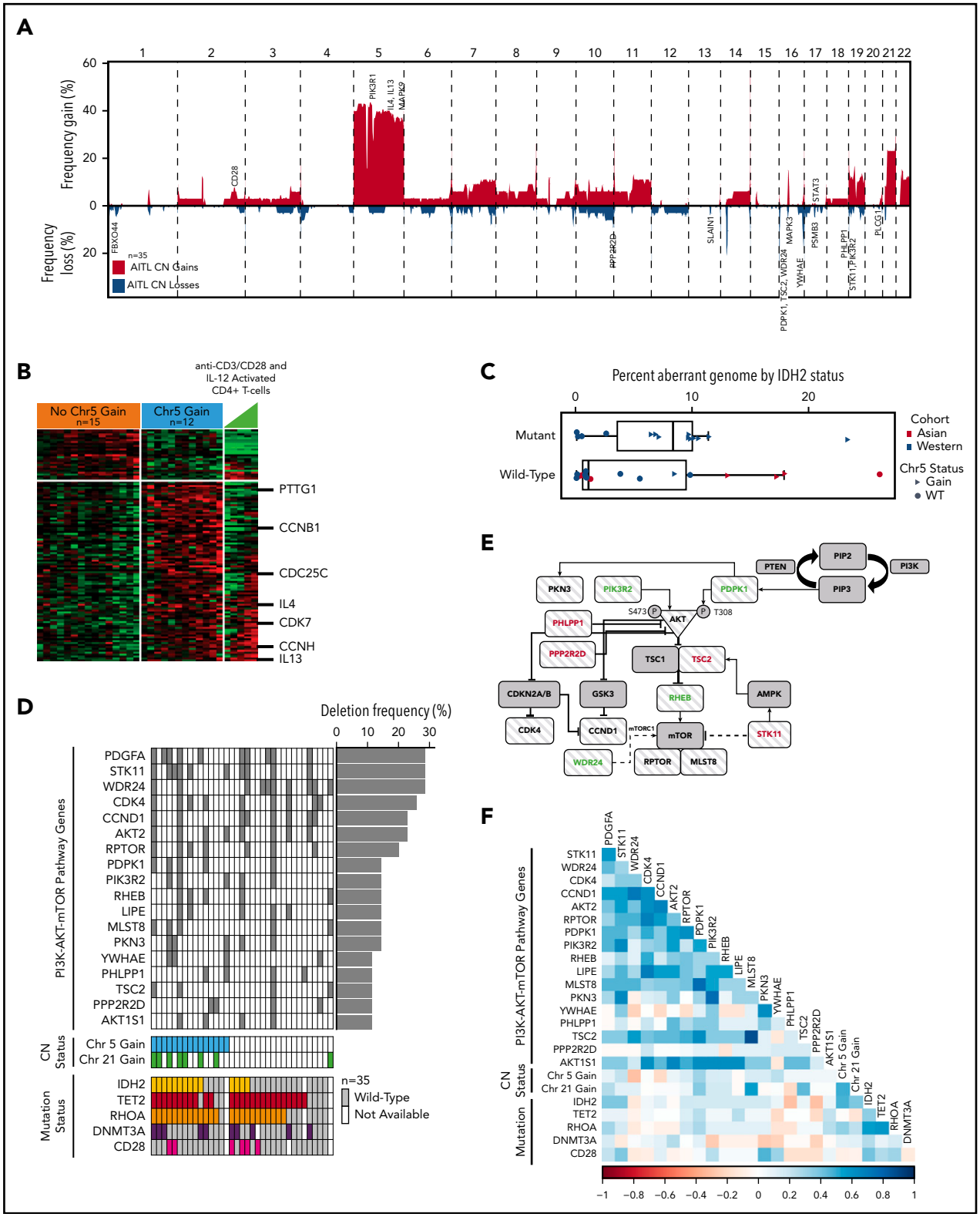

Figure 2. CN analysis in AITL. (A) Frequency of chromosomal gains and losses in AITL tumors quantified using Nexus Copy Number. Candidate genes within aberrant loci are indicated. (B) Heat map of differentially expressed genes ($P < .05$) located on chr5 between cases with and without a chr5 gain. (C) Percent aberrant genome segregated on mutation status of *IDH2*^{R172} in AITL cases. Asian and Western cohorts are distinguished by color, whereas CN state of chr5 is indicated by shape. (D) Genes involved in the PI3K–AKT–mTOR pathway that are deleted in ≥10% of AITL cases and their association with frequent CNAs and mutations, which are indicated below. (E) PI3K–AKT–mTOR schematic diagram with striped patterned genes deleted in AITL at a frequency ≥ 10%. Genes in red are negative regulators, and genes in green are positive regulators. (F) Matrix of Pearson correlation coefficients for co-occurring genomic abnormalities and mutations in AITL.

Downloaded from http://ashpublications.org/blood/article-pdf/133/15/1664/1553089/blood872549.pdf by guest on 29 April 2025

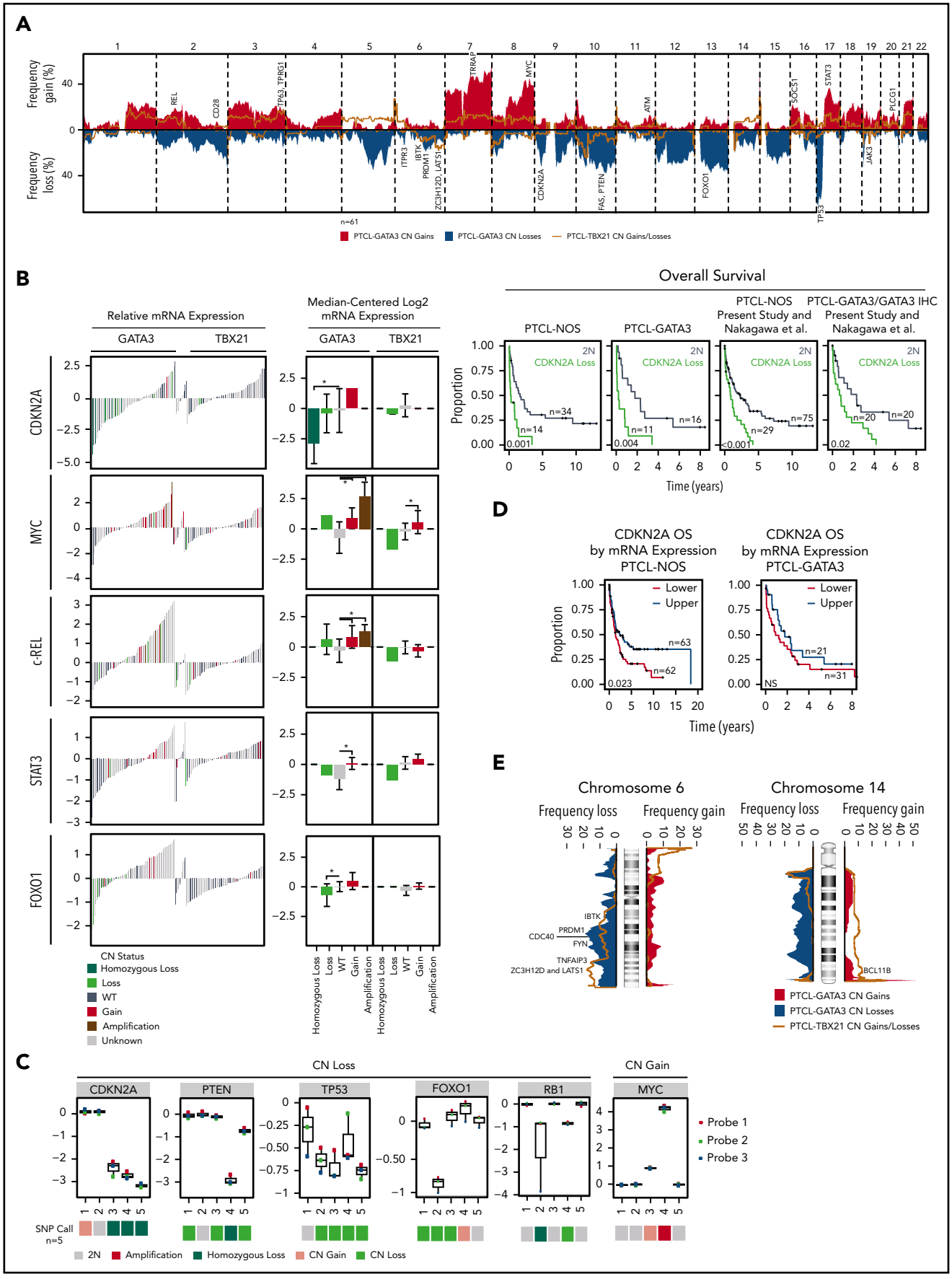

Figure 3.

Downloaded from http://ashpublications.org/blood/article-pdf/133/15/1664/1553089/blood872549.pdf by guest on 29 April 2025

Of the most frequent CNAs (Figure 2A), chromosome 5 (chr5) gain (43%; 15/35) and chr21 gain (23%; 8/35) significantly co-occurred ($P = .01$). Gain of chr7/7q, chr11, chr19, or chr22q occurred in ≥10% (4/35) of AITL cases, consistent with a recent study.[17] Integration of CN status and GEP data identified 597 upregulated ($P < .05$) candidate target genes, which were enriched in biological processes involving RNA/protein metabolism, mitochondrial dysfunction, and cell cycle regulation using DAVID analysis (supplemental Table 4).

Chr5 gain in AITL is distinctive, because other hematological malignancies exhibit chr5 loss.[26,27] Examination of chr5 genes in cases with GEP showed that 95 were significantly ($P \leq .05$) upregulated in the cases with chr5 gain, including *IL4*, *IL13*, and *MAPK9*, which affect cell cycle regulation and T-cell differentiation.[28] Many of these genes showed an expression pattern similar to *IL12*-activated normal $CD4^+$ T cells (Figure 2B). Genes related to cell cycle ($P = .004$; false discovery rate [FDR], 4.21%) and T-cell activation ($P = .035$; FDR, 24.0%) were also significantly upregulated in cases with chr5 gain (supplemental Table 5). Gene-set enrichment analysis indicated marginal enrichment of oxidative phosphorylation–associated genes ($P = .048$; FDR = not significant [NS]). Chr5 gain was significantly associated with $IDH2^{R172}$ mutation ($P = .01$) but not with recurrent mutations in *DNMT3A*, $RHOA^{G17V}$, or *TET2*. AITL cases without chr5 gain showed enrichments of NF-κB ($P = .009$, FDR, 11.1%) and PI3K-AKT ($P = .008$; FDR, 0.47%) pathway signatures according to DAVID, suggesting alternative oncogenic pathways in these cases (supplemental Table 6). A similar gene-signature association was observed in $IDH2^{WT}$ cases. Interestingly, a marginally higher percent aberrant genome was associated with $IDH2^{R172}$ mutation in AITL (Figure 2C).

Compared with the entire chromosome/arm gains, more focal deletions were observed and included a number of loci located at 1p36.33, 9q34.11, 13q22.3, 16p13.3, 16q24.3, 17p13.1, and 19q13.2-4. We identified frequently deleted genes (≥10%, 4/35) and analyzed only genes expressed (≥ 1 fragments per kilobase of transcript per million mapped reads) in normal T_{FH} cells.[29] Genes in deleted loci having significant loss of mRNA expression included genes involved with ubiquitylation/proteolysis (*FBXO44* and *PSMB3*), microtubule organization (*SLAIN1*), and mitoribosome stability (*MRPL28* and *MPV17L2*). Association with the PI3K–AKT–mTOR pathway was observed in genes lost in ≥4 cases (supplemental Table 7) and included negative regulators (*STK11*, *PPP2R2D*, *PHLPP1*, and *TSC2*),[30] PI3K regulatory subunit *PIK3R2* (p85β), and genes regulating amino acid sensing in the mTORC1 signaling pathway (*WDR24*) (Figure 2D-E). The positive regulator of PI3K-AKT signaling, *PDPK1*[30] (16p13.3), which is mutated in 6% of AITL,[9] is also deleted in AITL. CN loss of several PI3K-AKT phosphatases (*PHLPP1* and/or *PPP2R2D*) showed a trend of mutual exclusivity with $IDH2^{R172}$ mutations ($P = .057$; CoMEt_exact_test[31]), whereas *DNMT3A* mutations showed a negative correlation with other key regulators of the PI3K-AKT pathway, with some genes showing a marginal trend (eg, *PIK3R2 and PKN3*; $P = .08$), whereas other genes (eg, *STK11*, *YWHAE*, and *PPP2R2D*; $P = .12$ to $.26$) did not show statistical significance, probably because of the small number of cases available for analysis. These findings suggest alternative oncogenic mechanisms in mutant cases (Figure 2F). Examination of TCR signaling showed that 12% of AITL had *CD28* gain/amplification, in addition to mutations and fusions observed in AITL.[9,32,33]

Integrated genomic analysis of molecularly defined PTCL subgroups

PTCL-GATA3 exhibited a more aberrant genome (mean, 23%) than PTCL-TBX21 (mean, 8%; $P < .001$) (Figure 1D), with frequent partial/complete chr7 gain (48%; 15/31), partial/complete chr8q gain (45%; 14/31), and chr17q gain (42%; 13/31) (Figure 3A). *MYC* (8q24.21) was gained/amplified in 52% (16/31) with concomitant higher mRNA expression (3.7-fold; $P < .001$) (Figure 3B), along with an enrichment of *MYC* target genes ($P < .05$; FDR < 10%).[8] Chr17q gain encompassed *STAT3* and was associated with elevated mRNA (2.4-fold, $P < .001$) (Figure 3B). Interestingly, 9 of 11 cases with a *STAT3* gain had an *MYC* gain. Evaluation of MYC and phosphorylated STAT3 expression by IHC in available cases indicated a trend of higher protein expression with CN gain (supplemental Figure 3). Focal gain/amplification encompassing *REL* (2p16.1) was associated with increased mRNA (2.5-fold, $P = .005$) (Figure 1A-B; supplemental Figure 3B).

CN deletions in PTCL-GATA3 included deletion of chr17p (del-17p), del-13q, del-10q, del-9p21.3, del-5q, del-6q21, and del-1q, which affected well-characterized tumor suppressors (TSs) (*TP53* [58% heterozygous], *PTEN* [35%; 10 heterozygous, 1 homozygous], *FAS* [32%; 8 heterozygous, 2 homozygous], *CDKN2A/B* [45%; 7 heterozygous, 7 homozygous], and *PRDM1* [23%; heterozygous]). Of these, *CDKN2A* ($P = .03$) and *FOXO1* ($P = .02$) mRNA significantly decreased with CN deletion (Figure 3B). Several genes within CNAs were validated using an nCounter Cancer CN Assay (Figure 3C). *CDKN2A* loss was associated with poorer OS in the PTCL-NOS ($P = .001$) and PTCL-GATA3 ($P = .004$) (Figure 3B) subgroups. *PTEN* and *TP53* loss and *MYC* and *STAT3* gain demonstrated a trend of inferior OS in PTCL-NOS, but these likely reflect the inferior survival of PTCL-GATA3 compared with PTCL-TBX21, because these CNAs are more common in PTCL-GATA3 (supplemental Figure 4). We validated OS associations of *CDKN2A* in combination with an independent series[23] and observed similar survival trends (Figure 3B). Furthermore, low *CDKN2A* mRNA expression associated with poor OS in the series of PTCL-NOS ($P = .007$) and a trend in PTCL-GATA3 (Figure 3D). Genes within aberrant loci were significantly enriched in biological processes

Figure 3. CN and expression analysis in molecular subgroups of PTCL. (A) Frequency of chromosomal gains and losses found in PTCL-GATA3 and PTCL-TBX21 tumors. Candidate genes in focal regions are indicated. (B). The relative mRNA expression (n = 157, previously molecularly classified PTCL-NOS[7,8]) and median-centered log2 mRNA expression (n = 47, CN cases with Affymetrix HG-U133 Plus2 gene expression data) of select recurrently aberrant genes with differential gene expression relative to DNA CN status. In the relative mRNA expression plots (left panel), colored bars (except gray) indicate cases included in the present CN analysis. Kaplan-Meier curves comparing specific gene aberrations in the PTCL-NOS entity, PTCL-GATA3 subgroup, and combined with a previously published PTCL-NOS series[23] are included for *CDKN2A*, which tended to be associated with poor OS. (C) Validation of genes within recurrent loci observed in the PTCL-GATA3 subgroup using the NanoString Cancer CNV assay. (D) Kaplan-Meier curves comparing the upper vs lower halves of *CDKN2A* mRNA expression from all molecular PTCL-NOS cases with GEP and outcome data (n = 125) from (B) (left panel) and only in PTCL-GATA3 (n = 52; right panel). (E) Frequency plots of chr6 and chr14 alterations, which have differential regions of abnormality in PTCL-GATA3 and PTCL-TBX21 subgroups. Candidate target genes within the regions are noted.

Downloaded from http://ashpublications.org/blood/article-pdf/133/15/1664/1553089/blood872549.pdf by guest on 29 April 2025

involving splicing, ubiquitination, and signaling pathways (PI3K/mTOR, FAS, and TCR). When mRNA expression of these genes was examined, the expected changes in expression were observed (supplemental Table 8).

PTCL-TBX21 had fewer CNAs and a less aberrant genome (8%), with 23% of cases having gains along the q-arms of chr1 and chr3. These loci included immune-regulatory genes (*CD244*, *CD247*, *FASLG*) at chr1q23 and cell cycle regulators (*TP63*, *TPRG1*) at chr3q28, with significantly increased mRNA expression ($P < .05$) in cases with a respective CN gain. Six cases (20%) had a gain encompassing *BCL11B* (14q32.2; Figure 3E), a negative regulator of *GATA3* and the T_H2 expression program.[34] Five cases (17%) showed *BCL6* gain at 3q27.3 but did not show any change in mRNA expression. Recurrent losses were infrequent compared with PTCL-GATA3, but focal deletions were observed on chr6, chr10, chr16, chr17, and chr19. chr6q was affected by deletions in PTCL-GATA3 and PTCL-TBX21; however, the deletions were more telomeric in PTCL-TBX21 (Figure 3D) and included newly identified TS-related (*LATS1* and *ZC3H12D*) or TCR-related (*FYN* and *IBTK*) genes and *TNFAIP3*, with concordant low mRNA expression associated with CN deletion. Chr10 deletion included the proapoptotic gene *BNIP3*, T_H2-related gene *PRKCQ*,[35] and cell polarity–related gene *PARD3*. Genes within CNAs were enriched in cytotoxicity-mediating pathways and processes related to RNA splicing (supplemental Table 9).

Because a cytotoxic $CD8^+$ T-cell group[7,8] was predominantly enriched in PTCL-TBX21,[8] we examined a $CD8^+$ cytotoxic GEP signature[36] and corresponding CN data. We observed that cases with a high cytotoxic signature tended to be more aberrant (supplemental Figure 5).

Validation of subgroup-specific CNAs and comparative analysis with other major PTCL entities

Because genomic profiles were distinct between PTCL-GATA3 and PTCL-TBX21, we examined whether CNAs could delineate these 2 subgroups. Using unsupervised HC of CNAs present in ≥10% of either PTCL-GATA3 or PTCL-TBX21, we observed 2 distinct clusters enriched in PTCL-GATA3 or PTCL-TBX21 cases. Analysis of genomic CN profiles from 2 available PTCL-NOS cohorts[22,23] showed similar abnormalities (supplemental Figure 1C-D), with 2 major HC clusters of cases characterized by similar CNAs (data not shown). Expression of *CCR4* (*GATA3* target gene) and *CXCR3* (*TBX21* target gene)[37] was available in 1 series[23] and was used as surrogate markers for the 2 subgroups, because GATA3/CCR4 and TBX21/CXCR3 showed a positive correlation at the protein and mRNA levels (Figure 4A-B).[38] The $CCR4^+$ group had a higher than average aberrant genome compared with $CXCR3/CCR3^+$ cases, an observation concordant with PTCL-GATA3 vs PTCL-TBX21 (Figure 4C). Meta-analysis of all series (n = 159) showed distinct clusters with comparable percent aberrant genome distributions and enrichment in either of the molecular subgroups with significant differences in CNAs (Figure 4D). This large cohort allowed for correlative association of CNAs. *TP53* loss significantly (Fisher's exact test) co-occurred with loss of *PTEN* ($P < .001$), *PRDM1* (0.002), and *CDKN2A* ($P < .001$), but it had no or a negative correlation with CNAs present in PTCL-TBX21 (Figure 4E).

We compared the AITL, PTCL-TBX21, and PTCL-GATA3 genomic profiles with other PTCL entities (Figure 5A-B), including ALCL,[20] ATLL,[19] and systemic CTCL.[21] PTCL-TBX21 has a low-complexity genome similar to AITL, whereas PTCL-GATA3 showed a highly aberrant genome more comparable to ATLL and ALK^- ALCL (Figure 5C). Several CNAs were distinct among entities (Figure 5D). Co-occurring gains of chr5 and chr21 were unique to AITL. *CDKN2A*, *PRDM1*, and *TP53* deletions were comparable between PTCL-GATA3 and ATLL, but *PTEN* deletions were uncommon in ATLL.[19] Del-5q, del-9, del-12, del-13q, del-15q, and chr7 gain were more frequently associated with PTCL-GATA3. PTCL-TBX21 had few CNAs; the most recurrent were del-10p and chr1q gain, the latter of which was also observed in ATLL, ALCL, and PTCL-GATA3 but not in AITL or CTCL.[19-21]

Mutational analysis of PTCL subgroups

Mutation analysis of genes within aberrant loci was performed in 31 PTCL molecular-subgroup cases and 5 PTCL-T_{FH} cases (Figure 6A). Amplicon-sequencing data of 4 genes (*CD28*, *DNMT3A*, *RHOA*, and *TET2*) from a previous study[39] were available in 9 cases. One hundred percent concordance in variant calls was observed with the custom-capture platform, demonstrating adequate coverage and robustness in variant calling.

TP53 mutations were associated with PTCL-GATA3 (5/17) and co-occurred with CN loss (Figure 6A); thus, aberrant *TP53* signaling due to mutation and CN deletion was significantly associated with PTCL-GATA3 (Fisher's exact test, $P < .001$). *TP53* mutations occurred in the DNA binding and tetramerization domains, including the hotspot $TP53^{R175H}$ (n = 2) (Figure 6B). These aberrations did not show association with mRNA expression. Other DNA repair or *TP53* signaling genes (*ATM* and *TRRAP*) were mutated in both subgroups. *PRDM1* mutations identified in the PTCL-GATA3 subgroup co-occurred with CN deletion. Despite recurrent deletions in other TSs (*FOXO1* and *PTEN*), mutations were infrequent or absent; as expected, no mutation in *CDKN2A* was observed due to biallelic deletions. Other genes with CNAs were involved in JAK-STAT (*SOCS1* and *JAK3*), PI3K-AKT (*ITPR3* and *ITPKB*), and T-cell activation (*PLCG1*, *PTPRC*, *FYN*, and *VAV1*) and were mutated, with no significant difference between the subgroups (Figure 6A).

Mutations in the DNA methylation regulator *TET2* were observed at near-equal frequencies in PTCL-GATA3 (4/17) and PTCL-TBX21 (3/11), but *TET1*, *TET3*, and *DNMT3A* mutations were enriched in PTCL-TBX21 (4/11 vs 2/17). Histone methyltransferases showed a similar mutation frequency (Figure 6A). An uncommon $IDH2^{R172W}$ variant was observed in 1 PTCL-TBX21 case, which harbored an $RHOA^{G17V}$ mutation and a *DNMT3A* mutation but lacked a PTCL-T_{FH} immunophenotype upon IHC examination. Interestingly, *DNMT3A* mutations in PTCL-TBX21 were restricted to the MTase motif of the catalytic domain and affected $DNMT3A^{R882}$ (2/2), which was also observed in our larger cohort,[39] in contrast to AITL, in which only 1 of 22 cases showed $DNMT3A^{R882}$ mutation (Figure 6C). PTCL-T_{FH} cases showed a mutation profile closer to AITL cases,[9,40] but without *IDH2* mutation. A mutation of *TET3* co-occurring with *TET2* and *BCL11B* gain was present in 1 case; however, too few cases were studied for a definitive assessment (Figure 6A).

Downloaded from http://ashpublications.org/blood/article-pdf/133/15/1664/1553089/blood872549.pdf by guest on 29 April 2025

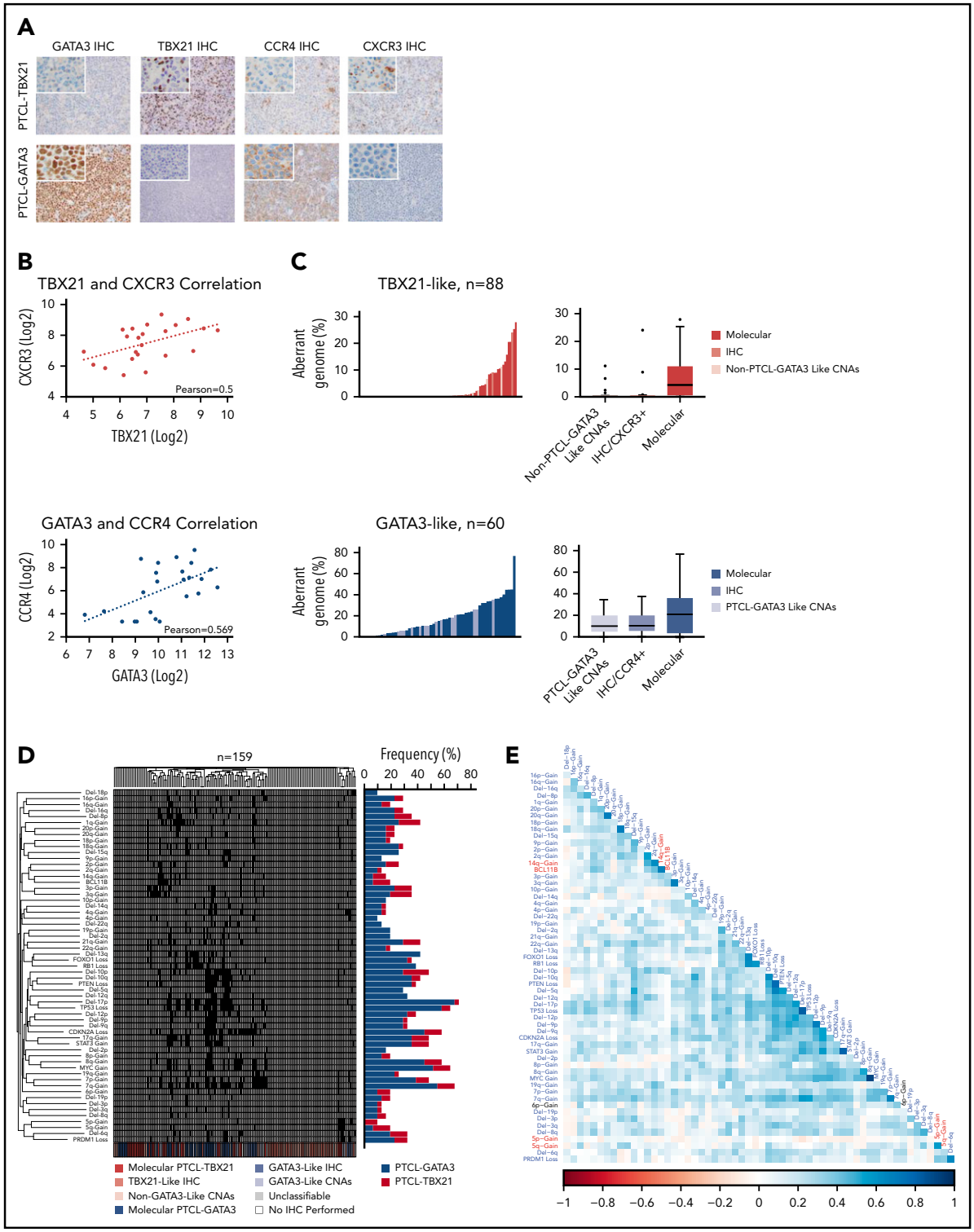

Figure 4. Unsupervised HC of CNAs in PTCL. (A) IHC staining of GATA3, TBX21, CCR4, and CXCR3 in a molecularly classified case of PTCL-TBX21 (upper panels) or PTCL-GATA3 (lower panels). Original magnification of ×200 with an inset magnification of ×400. (B) Positive correlation of *TBX21* and *CXCR3* mRNA expression in the PTCL-TBX21 subgroup (upper panel) and *GATA3* and *CCR4* mRNA expression in the PTCL-GATA3 subgroup (lower panel). (C) Histograms (left panels) and boxplots (right panels) of the percent aberrant genome of PTCL-GATA3 and PTCL-TBX21 molecularly classified cases, along with PTCL-GATA3–like and PTCL-TBX21–like cases, from 2 published series.[22,23] (D) Unsupervised HC of 3 PTCL-NOS series[22,23] by recurrent CNAs observed in the PTCL-GATA3 or PTCL-TBX21 molecular subgroups at a frequency ≥10%. The molecular PTCL-GATA3/GATA3–like cases (blue shades) dominate the central clusters, whereas the outside clusters, which tend to lack frequent CNAs, are predominately molecular PTCL-TBX21/TBX21–like cases (red shades). The frequency of these aberrations in the molecularly classified PTCL-NOS subgroups from the present study are depicted to the right of the cluster. (E) Matrix of Pearson correlation coefficients for co-occurring CNAs. Abnormalities depicted in blue type are more frequent in PTCL-GATA3, whereas abnormalities depicted in red type are more frequent in PTCL-TBX21. The black type (6p-Gain) represents a CNA that was observed at near-equal frequencies in the 2 molecular subgroups.

Downloaded from http://ashpublications.org/blood/article-pdf/133/15/1664/1553089/blood872549.pdf by guest on 29 April 2025

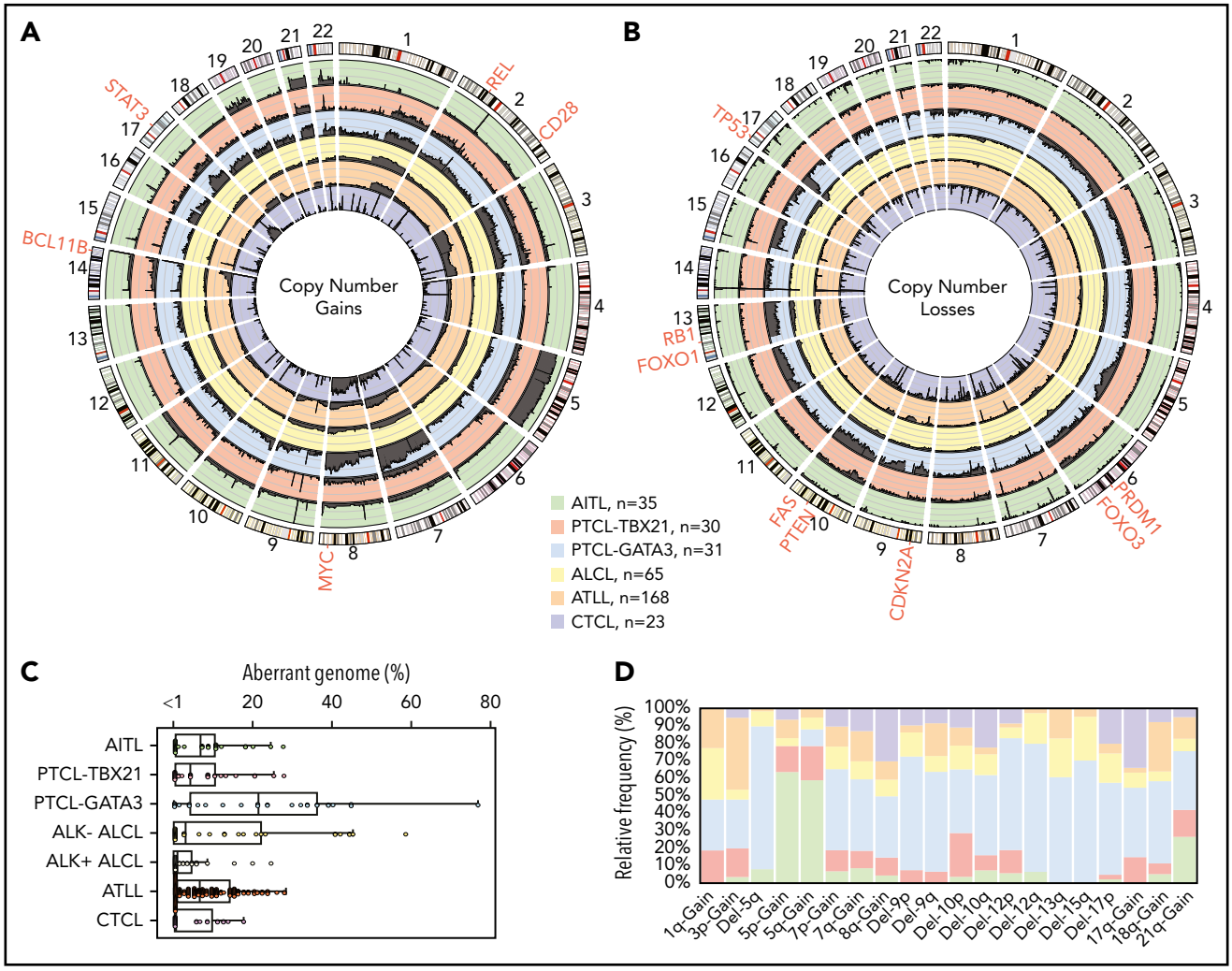

Figure 5. Comparison of CNAs found in PTCL entities/subgroups. Circos plots comparing the frequency of gains (A) and losses (B) found in PTCL entities/subgroups (AITL, PTCL-TBX21, PTCL-GATA3, ALCL, ATLL, and CTCL). The dark gray shading denotes aberrant regions. The scale lines represent 20% increments. (C) Boxplot of the aberrant genome in PTCL entities/subgroups. The dot plot overlay represents the aberrant genome of individual samples separated into 1% bins. (D) Relative frequency distribution of CNAs presenting at a frequency ≥25% in ≥1 PTCL entity or subgroup.

Discussion

Comprehensive genetic characterization of AITL and newly defined PTCL-NOS molecular subgroups validated their distinct genetic evolution and identified potential therapeutic targets. Although we used well-characterized cases supported by GEP and pathology review, there is still the possibility that the frequency of aberrations of some of the molecular entities may be underestimated due to low tumor content cases, which is commonly observed in many PTCLs. However, major CNAs in AITL were consistent with previous cytogenetic and array-comparative genomic hybridization (aCGH) studies.[17,41,42] However, integrative analysis with GEP revealed that genetic changes targeted oncogenic pathways not previously identified.[41-44] Comparative analysis with other major WHO-defined PTCL entities showed that AITL harbors a minimally aberrant genome. chr5 gain (43%) co-occurring with chr21 gain and *IDH2*^{R172} mutation were specifically associated with AITL. Contrary to previous studies,[41,42] trisomy 3 was infrequent (1/35). This discrepancy in chr3 gain was noted in an earlier cytogenetic study (interphase 78% vs metaphase 41%)[45] and also was not observed in a recent aCGH study,[17] although it is possible that trisomy 3 may be present in subclones and not detected by hybridization-based platforms.[44] Chr13q22 loss was observed in 14% (5/35), in agreement with previous findings,[44] and it may target *SLAIN1* (13q22.3), involved in microtubule reorganization. chr5 gain significantly co-occurred with chr21 gain, but the cooperative roles of these abnormalities are challenging to decipher, because they harbor epigenetic mutations and pleiotropic effects due to *IDH2*^{R172} mutation–induced increased 2-hydroxyglutarate (2-HG). 2-HG inhibits α-KG–dependent dioxygenases (eg, histone demethylases and the *TET* family of 5mC hydroxylases)[46] and can also promote the Warburg effect by directly competing with α-KG in the tricarboxylic acid cycle, thus altering the epigenetic and metabolic programs in T cells. *IDH2* mutation is associated with a more pronounced T_{FH} signature and T-cell activation via epigenetic modification[39] and tends to have a more aberrant genome compared with wild-type cases, possibly due to an inhibitory effect of 2-HG on DNA repair enzymes.[47] In contrast, *IDH2*^{WT} cases showed significant enrichment of PI3K-AKT activation pathways and had focal losses of negative regulators (phosphatases) of the PI3K-AKT pathway. Thus, constitutive

Downloaded from http://ashpublications.org/blood/article-pdf/133/15/1664/1553089/blood872549.pdf by guest on 29 April 2025

Figure 6. Select CNAs or genes found to be recurrently mutated in molecular PTCL subgroups. (A) The block color represents the type of mutation. Blocks with 2 colors indicate that >1 type of mutation was observed in the case. CNA status of the mutated genes are noted (3 = copy gain, 4 = amplification, 1 = copy loss, 0 = homozygous copy loss). The bar graphs to the right of the plot indicate the number of cases with the denoted mutation or CNA. The total percent aberrant genome is indicated below the plot. *Denotes 3 cases that were only included for mutation analysis, and CN status was determined by CopywriteR.[61] Schematic diagrams of the location of coding mutations identified in *TP53* (B) and *DNMT3A* (C). The *DNMT3A* schematic diagram combines targeted sequencing results from this study with previous amplicon sequencing data.[39] The figures were generated using MutationMapper.[62] MTase, methyltransferase.

Downloaded from http://ashpublications.org/blood/article-pdf/133/15/1664/1553089/blood872549.pdf by guest on 29 April 2025

activation of the PI3K-AKT pathway or impairment of the DNA repair pathway and disturbed metabolic pathways may be unique vulnerabilities that can be exploited in AITL, depending on the mutational status of *IDH2*. Wild-type cells may show a more sensitive response to PI3K-mTOR inhibitors, whereas *IDH2*-mutant cells may be particularly sensitive to alkylating agents,[47] and PARP inhibitors may have synergistic effects.

According to the recent WHO classification of lymphoid tumors,[1] PTCL-T_{FH} is now included as a provisional entity of T-cell lymphoid neoplasms. In concordance with a previous study,[17] we observed differences in the CN profiles of PTCL-T_{FH} and AITL: specifically, chr5 gain is infrequent in PTCL-T_{FH}, whereas loss of chr6q and chr1q gain are more common (supplemental Figure 1E). The mutation profile of PTCL-T_{FH} identified mutations in *TET2*, *DNMT3A*, and *RHOA*, which are also common in AITL; however, we did not observe $IDH2^{R172}$ mutations, consistent with previous reports.[9,48] Although the number of PTCL-T_{FH} cases studied to date is small, the data suggest that PTCL-T_{FH} may be a genetically distinct entity from AITL.

We provided evidence that novel molecular subgroups[8] evolve by distinct genetic pathways and are characterized by distinct genomic complexity. By GEP, PTCL-GATA3 represents a subgroup distinct from PTCL-TBX21, which may contain a non-cytotoxic and a cytotoxic subgroup characterized by $CD8^+$ T cells.[8] CNAs support the GEP classification, because PTCL-GATA3 showed high genomic complexity with frequent CNAs of well-known TSs and oncogenes, some with functional consequences observed at the mRNA level and inferior survival, which are in agreement with earlier studies.[8,15] A recent study demonstrated that PTCL-NOS cases classified as GATA3 expressing on a different platform trended toward poorer OS.[49] In contrast, PTCL-TBX21 had low genomic complexity and did not show prominent TS deletions and mutations. *TP53* signaling was a primary target in >50% of PTCL-GATA3 cases by biallelic deletion/mutation of TP53, *CDKN2A/2B* ($p14^{ARF}$/$p16^{INK4A}$), or *RB1*. $P14^{ARF}$ is a negative regulator of *TP53* signaling, and $p16^{INK4A}$ regulates the RB-mediated G_1 checkpoint. *CDKN2A* showed prognostic significance in PTCL-GATA3, but validation with additional cases is required. *PRDM1*, important in the homeostatic control of T-cell activation and proliferation, is likely the driver of del-6q21. *PRDM1* loss may promote the development of PTCL-GATA3. Remarkably, del-5q was exclusive to PTCL-GATA3, whereas chr5 gain and a focal 14q32 gain encompassing *BCL11B* were noted more frequently in PTCL-TBX21. *BCL11B* is critical in T-cell differentiation at the double-negative 3/4 stage by preventing differentiation of early T cells into natural killer cells and other innate immune cell lineages, in part by repressing *GATA3* expression.[34] However, its role in the lymphomagenesis of PTCL-TBX21 is unclear. Genes regulating NF-κB signaling (*ZC3H12DC*/p34[50] and *TNFAIP3*) and TS kinase (*LATS1*) were more frequently lost in PTCL-TBX21. Genomic losses observed in PTCL-TBX21 targeted genes associated with cell-mediated cytotoxicity and cellular processes involving metabolic reprogramming.[51] A meta-analysis of 2 additional PTCL-NOS cohorts[22,23] demonstrated that subgroup-associated CNA profiles can be validated and delineated independently, as is evident by the clustering of percent aberrant genome, specific CNA association with clinical outcome data, and/or expression of *GATA3* and *TBX21* target genes (*CCR4* and *CXCR3*, respectively). Although many of the CNAs are significantly associated with a specific subgroup, as shown in Figure 5, with the exception of *TP53* loss (~50%), the majority of these CNAs do not exceed 25% to 30% and, thus, may not be usable per se as molecular subgroup classifiers; rather, they may aid in the molecular diagnosis in challenging PTCL-NOS cases.

Although *MYC–CDKN2A–TP53* signaling axis deregulation is often observed in NHLs, co-occurrence of impaired *TP53* signaling and *PTEN* loss is uncommon in neoplasms, because studies have shown that functional interdependence and mutations are often mutually exclusive.[52] *TP53* directly regulates *PTEN* mRNA expression[53] and *PTEN* stabilizes *TP53* by inhibiting *MDM2* translocation to the nucleus[54] and can directly bind and stabilize *TP53* in the nucleus.[55] *TP53* and *PTEN* codeletions are significantly associated with PTCL-GATA3 but not with PTCL-TBX21 or other T-cell NHLs. Thus, their cooperative role in T-cell lymphomagenesis warrants further investigation. We noted mutual exclusivity of *TP53* loss and *TET1/2/3* mutations, suggesting that epigenetic alterations due to *TET* deficiency and *TP53* functional impairment may lead to distinct clonal evolution.

Recently, Horwitz et al showed clinical efficacy of a PI3K-δ,γ inhibitor (duvelisib) in a phase 1 trial of PTCL-NOS patients.[56] Because of the promising response in this clinical trial and preclinical models,[56] it would be essential to precisely classify PTCL cases and their genomic abnormalities for correlative studies for future multi-institutional clinical trials. Many of the CNAs (deletions of *PTEN*, *STK11*, and *TSC2* and/or *MYC* amplification) likely converge to constitutively activate PI3K–AKT–mTOR signaling.[30] The mTOR pathway is critical for the integration of costimulatory, cytokine, environmental, and metabolic cues necessary for T-cell differentiation,[57] T-helper cell polarization,[58] and proliferation.[59] *TP53* negatively regulates mTOR pathways via *PTEN*-AKT and the *TSC2*-AMPK β1 axis.[60] Although preliminary, we observed that mTOR signaling pathways can be a promising target for therapeutic intervention using a number of T-cell lines (supplemental Figure 6). Because these T-cell lines are not derived from AITL or PTCL-GATA3/TBX21, the findings will need to be validated and more specifically defined using authentic PTCL cell lines or xenograft models when available.

In summary, the complexity of PTCL can be addressed with greater clarity with the integration of global genomic analyses. This study provides further evidence of the existence of the 2 separate subgroups (PTCL-GATA3 and PTCL-TBX21) previously identified[8] within the PTCL-NOS group, and it has identified genetic features that are distinct between the 2. AITL cases showed a CN profile different from these 2 subgroups, and the *IDH2*-mutated group exhibited unique features that may indicate exploitable therapeutic vulnerabilities.

Acknowledgments

The authors thank the University of Nebraska Medical Center Human Genetics Laboratory at the Munroe-Meyer Institute, Tissue Science Facility, Genomic Core Facility at City of Hope, SingHealth Tissue Repository, Advanced Molecular Pathology Laboratory at SingHealth, and Duke–National University of Singapore (NUS) Genome Biology Facility. The authors also thank Francoise Berger for contribution of cases to the International Peripheral T-Cell Lymphoma Consortium.

Downloaded from http://ashpublications.org/blood/article-pdf/133/15/1664/1553089/blood872549.pdf by guest on 29 April 2025

The work was supported in part by City of Hope Lymphoma Specialized Programs of Research Excellence grant P50 CA107399 and National Institutes of Health (NIH) National Cancer Institute (NCI) grant P30 CA033572. Partial support is from NIH NCI Eppley Cancer Center Support grant P30 CA036727, NIH National Center for Research Resources grant 5P20RR016469, and NIH National Institute for General Medical Science grant 8P20GM103427 (G.B.). F.B. is supported by Oncosuisse grant KLS-02403-02-2009, Anna Lisa Stiftung, and The GELU Foundation. J.I. is supported by the Leukemia and Lymphoma Society (TRP-6129-04), NIH NCI Eppley Cancer Center Support grant P30 CA036727 and NIH NCI grants UH2 CA206127 02 and P01 CA229100 01. W.C.C. is supported by NIH NCI Strategic Partnering to Evaluate Cancer Signatures (SPECS) II 5 UO1 CA157581-01, NIH NCI Specialized Programs of Research Excellence 1P50 CA136411-01 01A1 PP-4, and City of Hope internal funds. C.K.O. is supported by Singapore Ministry of Health's National Medical Research Council, the Tanoto Foundation, New Century International Pte. Ltd., the Ling Foundation, Singapore National Cancer Centre Research Fund, and Oncology Academic Clinical Program (ONCO-ACP) Cancer Collaborative Scheme. The University of Nebraska DNA Sequencing Core receives partial support from NIH National Center for Research Resources (1S10RR027754-01, 5P20RR016469, RR018788-08) and NIH National Institute for General Medical Science (8P20GM103427, GM103471-09).

Authorship

Contribution: T.B.H., A.B., J.Y., W.L., C.L., W.C.C., and J.I. designed and performed the research; T.B.H., A.B., W.L., Q.G., and W.Z. analyzed and/or interpreted the data; Y.L., B.J.D., and J.M.S. collected data; M.-L.N., C.A., T.C.G., J.V., D.D.W., C.W., K.F., S.T.L., C.K.O., R.D.G., E.M., F.L., C.H., S.H., M.B.P., M.A.L., R.A.W., B.T.T., N.Y., K.O., M.S., A.R., G.O., E.C., L.M.R., E.S.J., R.M.B., F.d'A., G.I., F.B., L.M.S., L.d.L., P.G., T.W.M., S.P., and W.C.C. provided materials, conducted the pathological review, and/or contributed clinical/aCGH/GEP data; and T.B.H., A.B., and J.I. wrote the manuscript.

Conflict-of-interest disclosure: The authors declare no competing financial interests.

ORCID profiles: E.M., 0000-0001-9221-0117; F.B., 0000-0001-5637-8983.

Correspondence: Javeed Iqbal, Department of Pathology and Microbiology, University of Nebraska Medical Center, Omaha, NE 68198-6842; e-mail:jiqbal@unmc.edu; and Wing C. Chan, Department of Pathology, City of Hope National Medical Center, Duarte, CA 91010; e-mail: jochan@coh.org.

Footnotes

Submitted 18 September 2018; accepted 10 February 2019. Prepublished online as *Blood* First Edition paper, 19 February 2019; DOI 10.1182/blood-2018-09-872549.

*T.B.H. and A.B. contributed equally to this work.

Contact Javeed Iqbal (jiqbal@unmc.edu) for original data, which will be deposited into the National Center for Biotechnology Information Gene Expression Omnibus database following publication.

The data were presented in part at the 58th annual meeting of the American Society of Hematology, San Diego, CA, 5 December 2016.

The online version of this article contains a data supplement.

The publication costs of this article were defrayed in part by page charge payment. Therefore, and solely to indicate this fact, this article is hereby marked "advertisement" in accordance with 18 USC section 1734.

Downloaded from http://ashpublications.org/blood/article-pdf/133/15/1664/1553089/blood872549.pdf by guest on 29 April 2025

REFERENCES

1. Swerdlow SH, Campo E, Harris NL, et al. WHO Classification of Tumours of Haematopoietic and Lymphoid Tissues. Vol. 2. Revised 4th ed. Lyon, France: International Agency for Cancer Research; 2017.
2. Vose J, Armitage J, Weisenburger D; International T-Cell Lymphoma Project. International peripheral T-cell and natural killer/T-cell lymphoma study: pathology findings and clinical outcomes. *J Clin Oncol*. 2008; 26(25):4124-4130.
3. Parrilla Castellar ER, Jaffe ES, Said JW, et al. ALK-negative anaplastic large cell lymphoma is a genetically heterogeneous disease with widely disparate clinical outcomes. *Blood*. 2014;124(9):1473-1480.
4. Federico M, Rudiger T, Bellei M, et al. Clinicopathologic characteristics of angioimmunoblastic T-cell lymphoma: analysis of the international peripheral T-cell lymphoma project. *J Clin Oncol*. 2013;31(2):240-246.
5. Xu B, Liu P. No survival improvement for patients with angioimmunoblastic T-cell lymphoma over the past two decades: a population-based study of 1207 cases. *PLoS One*. 2014;9(3):e92585.
6. de Leval L, Rickman DS, Thielen C, et al. The gene expression profile of nodal peripheral T-cell lymphoma demonstrates a molecular link between angioimmunoblastic T-cell lymphoma (AITL) and follicular helper T (TFH) cells. *Blood*. 2007;109(11):4952-4963.
7. Iqbal J, Weisenburger DD, Greiner TC, et al; International Peripheral T-Cell Lymphoma Project. Molecular signatures to improve diagnosis in peripheral T-cell lymphoma and prognostication in angioimmunoblastic T-cell lymphoma. *Blood*. 2010;115(5):1026-1036.
8. Iqbal J, Wright G, Wang C, et al; Lymphoma Leukemia Molecular Profiling Project and the International Peripheral T-cell Lymphoma Project. Gene expression signatures delineate biological and prognostic subgroups in peripheral T-cell lymphoma. *Blood*. 2014; 123(19):2915-2923.
9. Vallois D, Dobay MP, Morin RD, et al. Activating mutations in genes related to TCR signaling in angioimmunoblastic and other follicular helper T-cell-derived lymphomas. *Blood*. 2016;128(11):1490-1502.
10. Lemonnier F, Couronné L, Parrens M, et al. Recurrent TET2 mutations in peripheral T-cell lymphomas correlate with TFH-like features and adverse clinical parameters. *Blood*. 2012; 120(7):1466-1469.
11. Cairns RA, Iqbal J, Lemonnier F, et al. IDH2 mutations are frequent in angioimmunoblastic T-cell lymphoma. *Blood*. 2012;119(8): 1901-1903.
12. Couronné L, Bastard C, Bernard OA. TET2 and DNMT3A mutations in human T-cell lymphoma. *N Engl J Med*. 2012;366(1):95-96.
13. Odejide O, Weigert O, Lane AA, et al. A targeted mutational landscape of angioimmunoblastic T-cell lymphoma. *Blood*. 2014; 123(9):1293-1296.
14. Iqbal J, Weisenburger DD, Chowdhury A, et al; International Peripheral T-cell Lymphoma Project. Natural killer cell lymphoma shares strikingly similar molecular features with a group of non-hepatosplenic γδ T-cell lymphoma and is highly sensitive to a novel aurora kinase A inhibitor in vitro [published correction appears in *Leukemia*. 2011;25(8):1377]. *Leukemia*. 2011;25(2): 348-358.
15. Wang T, Feldman AL, Wada DA, et al. GATA-3 expression identifies a high-risk subset of PTCL, NOS with distinct molecular and clinical features. *Blood*. 2014;123(19):3007-3015.
16. Swerdlow SH, Campo E, Pileri SA, et al. The 2016 revision of the World Health Organization classification of lymphoid neoplasms. *Blood*. 2016;127(20):2375-2390.
17. Dobay MP, Lemonnier F, Missiaglia E, et al. Integrative clinicopathological and molecular analyses of angioimmunoblastic T-cell lymphoma and other nodal lymphomas of follicular helper T-cell origin. *Haematologica*. 2017;102(4):e148-e151.
18. Piccaluga PP, Fuligni F, De Leo A, et al. Molecular profiling improves classification and prognostication of nodal peripheral T-cell lymphomas: results of a phase III diagnostic accuracy study. *J Clin Oncol*. 2013;31(24): 3019-3025.
19. Yamagishi M, Nakano K, Miyake A, et al. Polycomb-mediated loss of miR-31 activates NIK-dependent NF-κB pathway in adult T cell leukemia and other cancers. *Cancer Cell*. 2012;21(1):121-135.
20. Boi M, Rinaldi A, Kwee I, et al. PRDM1/BLIMP1 is commonly inactivated in anaplastic large

T-cell lymphoma. *Blood*. 2013;122(15):2683-2693.

21. Lin WM, Lewis JM, Filler RB, et al. Characterization of the DNA copy-number genome in the blood of cutaneous T-cell lymphoma patients. *J Invest Dermatol*. 2012;132(1):188-197.

22. Hartmann S, Gesk S, Scholtysik R, et al. High resolution SNP array genomic profiling of peripheral T cell lymphomas, not otherwise specified, identifies a subgroup with chromosomal aberrations affecting the REL locus. *Br J Haematol*. 2010;148(3):402-412.

23. Nakagawa M, Nakagawa-Oshiro A, Karnan S, et al. Array comparative genomic hybridization analysis of PTCL-U reveals a distinct subgroup with genetic alterations similar to lymphoma-type adult T-cell leukemia/lymphoma. *Clin Cancer Res*. 2009;15(1):30-38.

24. Carter SL, Cibulskis K, Helman E, et al. Absolute quantification of somatic DNA alterations in human cancer. *Nat Biotechnol*. 2012;30(5):413-421.

25. Bouska A, Bi C, Lone W, et al. Adult high-grade B-cell lymphoma with Burkitt lymphoma signature: genomic features and potential therapeutic targets. *Blood*. 2017;130(16):1819-1831.

26. de Figueiredo AF, Capela de Matos RR, Othman MA, et al. Molecular cytogenetic studies characterizing a novel complex karyotype with an uncommon 5q22 deletion in childhood acute myeloid leukemia. *Mol Cytogenet*. 2015;8(1):62.

27. Fang J, Barker B, Bolanos L, et al. Myeloid malignancies with chromosome 5q deletions acquire a dependency on an intrachromosomal NF-κB gene network. *Cell Reports*. 2014;8(5):1328-1338.

28. Zhu J, Yamane H, Paul WE. Differentiation of effector CD4 T cell populations (*). *Annu Rev Immunol*. 2010;28(1):445-489.

29. Weinstein JS, Lezon-Geyda K, Maksimova Y, et al. Global transcriptome analysis and enhancer landscape of human primary T follicular helper and T effector lymphocytes. *Blood*. 2014;124(25):3719-3729.

30. Song MS, Salmena L, Pandolfi PP. The functions and regulation of the PTEN tumour suppressor. *Nat Rev Mol Cell Biol*. 2012;13(5):283-296.

31. Leiserson MD, Wu HT, Vandin F, Raphael BJ. CoMEt: a statistical approach to identify combinations of mutually exclusive alterations in cancer [published correction appears in *Genome Biol*. 2016;17(1):168]. *Genome Biol*. 2015;16(1):160.

32. Rohr J, Guo S, Huo J, et al. Recurrent activating mutations of CD28 in peripheral T-cell lymphomas. *Leukemia*. 2016;30(5):1062-1070.

33. Vallois D, Dupuy A, Lemonnier F, et al. RNA fusions involving *CD28* are rare in peripheral T-cell lymphomas and concentrate mainly in those derived from follicular helper T cells. *Haematologica*. 2018;103(8):e360-e363.

34. Califano D, Sweeney KJ, Le H, et al. Diverting T helper cell trafficking through increased plasticity attenuates autoimmune encephalomyelitis. *J Clin Invest*. 2014;124(1):174-187.

35. Marsland BJ, Soos TJ, Späth G, Littman DR, Kopf M. Protein kinase C theta is critical for the development of in vivo T helper (Th)2 cell but not Th1 cell responses. *J Exp Med*. 2004;200(2):181-189.

36. Newman AM, Liu CL, Green MR, et al. Robust enumeration of cell subsets from tissue expression profiles. *Nat Methods*. 2015;12(5):453-457.

37. Sundrud MS, Grill SM, Ni D, et al. Genetic reprogramming of primary human T cells reveals functional plasticity in Th cell differentiation. *J Immunol*. 2003;171(7):3542-3549.

38. Amador C, Greiner TC, Heavican T, et al. An immunohistochemistry algorithm subclassifies PTCL-NOS into gene expression profiling defined molecular subgroups with high accuracy. Paper presented at the 107th Annual Meeting of the United States and Canadian Academy of Pathology. 20 March 2018. Vancouver, BC, Canada.

39. Wang C, McKeithan TW, Gong Q, et al. IDH2R172 mutations define a unique subgroup of patients with angioimmunoblastic T-cell lymphoma. *Blood*. 2015;126(15):1741-1752.

40. Nguyen TB, Sakata-Yanagimoto M, Asabe Y, et al. Identification of cell-type-specific mutations in nodal T-cell lymphomas. *Blood Cancer J*. 2017;7(1):e516.

41. Nelson M, Horsman DE, Weisenburger DD, et al. Cytogenetic abnormalities and clinical correlations in peripheral T-cell lymphoma. *Br J Haematol*. 2008;141(4):461-469.

42. Schlegelberger B, Zwingers T, Hohenadel K, et al. Significance of cytogenetic findings for the clinical outcome in patients with T-cell lymphoma of angioimmunoblastic lymphadenopathy type. *J Clin Oncol*. 1996;14(2):593-599.

43. Fujiwara SI, Yamashita Y, Nakamura N, et al. High-resolution analysis of chromosome copy number alterations in angioimmunoblastic T-cell lymphoma and peripheral T-cell lymphoma, unspecified, with single nucleotide polymorphism-typing microarrays. *Leukemia*. 2008;22(10):1891-1898.

44. Thorns C, Bastian B, Pinkel D, et al. Chromosomal aberrations in angioimmunoblastic T-cell lymphoma and peripheral T-cell lymphoma unspecified: a matrix-based CGH approach. *Genes Chromosomes Cancer*. 2007;46(1):37-44.

45. Schlegelberger B, Zhang Y, Weber-Matthiesen K, Grote W. Detection of aberrant clones in nearly all cases of angioimmunoblastic lymphadenopathy with dysproteinemia-type T-cell lymphoma by combined interphase and metaphase cytogenetics. *Blood*. 1994;84(8):2640-2648.

46. Li Z, Cai X, Cai CL, et al. Deletion of Tet2 in mice leads to dysregulated hematopoietic stem cells and subsequent development of myeloid malignancies. *Blood*. 2011;118(17):4509-4518.

47. Wang P, Wu J, Ma S, et al. Oncometabolite D-2-hydroxyglutarate inhibits ALKBH DNA repair enzymes and sensitizes IDH mutant cells to alkylating agents. *Cell Reports*. 2015;13(11):2353-2361.

48. Manso R, González-Rincón J, Rodríguez-Justo M, et al. Overlap at the molecular and immunohistochemical levels between angioimmunoblastic T-cell lymphoma and a subgroup of peripheral T-cell lymphomas without specific morphological features. *Oncotarget*. 2018;9(22):16124-16133.

49. Sugio T, Miyawaki K, Kato K, et al. Microenvironmental immune cell signatures dictate clinical outcomes for PTCL-NOS. *Blood Adv*. 2018;2(17):2242-2252.

50. Liang J, Saad Y, Lei T, et al. MCP-induced protein 1 deubiquitinates TRAF proteins and negatively regulates JNK and NF-kappaB signaling. *J Exp Med*. 2010;207(13):2959-2973.

51. Mihaylova MM, Shaw RJ. The AMPK signalling pathway coordinates cell growth, autophagy and metabolism. *Nat Cell Biol*. 2011;13(9):1016-1023.

52. Trotman LC, Pandolfi PP. PTEN and p53: who will get the upper hand? *Cancer Cell*. 2003;3(2):97-99.

53. Stambolic V, MacPherson D, Sas D, et al. Regulation of PTEN transcription by p53. *Mol Cell*. 2001;8(2):317-325.

54. Mayo LD, Dixon JE, Durden DL, Tonks NK, Donner DB. PTEN protects p53 from Mdm2 and sensitizes cancer cells to chemotherapy. *J Biol Chem*. 2002;277(7):5484-5489.

55. Freeman DJ, Li AG, Wei G, et al. PTEN tumor suppressor regulates p53 protein levels and activity through phosphatase-dependent and -independent mechanisms. *Cancer Cell*. 2003;3(2):117-130.

56. Horwitz SM, Koch R, Porcu P, et al. Activity of the PI3K-δ,γ inhibitor duvelisib in a phase 1 trial and preclinical models of T-cell lymphoma. *Blood*. 2018;131(8):888-898.

57. Waickman AT, Powell JD. mTOR, metabolism, and the regulation of T-cell differentiation and function. *Immunol Rev*. 2012;249(1):43-58.

58. Delgoffe GM, Pollizzi KN, Waickman AT, et al. The kinase mTOR regulates the differentiation of helper T cells through the selective activation of signaling by mTORC1 and mTORC2. *Nat Immunol*. 2011;12(4):295-303.

59. Song J, Salek-Ardakani S, So T, Croft M. The kinases aurora B and mTOR regulate the G1-S cell cycle progression of T lymphocytes. *Nat Immunol*. 2007;8(1):64-73.

60. Feng Z, Zhang H, Levine AJ, Jin S. The coordinate regulation of the p53 and mTOR pathways in cells. *Proc Natl Acad Sci USA*. 2005;102(23):8204-8209.

61. Kuilman T, Velds A, Kemper K, et al. CopywriteR: DNA copy number detection from off-target sequence data. *Genome Biol*. 2015;16(1):49.

62. Vohra S, Biggin PC. Mutationmapper: a tool to aid the mapping of protein mutation data. *PLoS One*. 2013;8(8):e71711.

Downloaded from http://ashpublications.org/blood/article-pdf/133/15/1664/1553089/blood872549.pdf by guest on 29 April 2025